



doi:10.1016/S0016-7037(02)01318-2

Characteristics of alkenones synthesized by a bloom of *Emiliania huxleyi* in the Bering Sea

NAOMI HARADA,^{1,*} KYUNG HOON SHIN,² AKIHIKO MURATA,³ MASAO UCHIDA,¹ and TOMOKO NAKATANI⁴¹Mutsu Institute for Oceanography, Japan Marine Science and Technology Center, 690 Sekine, Mutsu 035-0022, Japan²Observational Frontier Research System for Global Climate Change/International Arctic Research Center, University of Alaska, Fairbanks, AK, USA³Ocean Research Department, Japan Marine Science and Technology Center, 2-15 Natsushima-cho, Yokosuka 237-0061, Japan⁴Marine Works Japan Ltd., Mutsuura, Kanazawa-ku, Yokohama 236-0031, Japan

(Received November 27, 2001; accepted in revised form October 29, 2002)

Abstract—We investigated the characteristics of the alkenones produced by a bloom of *Emiliania huxleyi* in the eastern Bering Sea in 2000. Alkenones were detected in surface waters between 57°N and 63°N, where phosphate concentrations were low and the ammonium/nitrate ratio was high. The total alkenone content ($C_{37:2}$, $C_{37:3}$, and $C_{37:4}$) ranged from 22.0 to 349 $\mu\text{g g}^{-1}$ in suspended particles and from 0.109 to 1.42 $\mu\text{g g}^{-1}$ in surface sediments. This suggests that a large proportion of the particulate alkenones synthesized in the surface water rapidly degraded within the water column and/or at the water-sediment interface of the Bering Shelf. The change in the stable carbon isotopic composition ($\delta^{13}\text{C}$) of $C_{37:3}$ alkenone could not be explained only by variation in $[\text{CO}_2(\text{aq})]$ in the surface water but also depended on the growth rate of *E. huxleyi*. The alkenone unsaturation index (U_{37}^{K}) was converted into an alkenone “temperature” with three equations (Prah1 et al., 1988; Sikes et al., 1997; Müller et al., 1998); Sikes et al.’s (1997) equation gave the best correlation with the observed sea surface temperature (SST) in the eastern Bering Sea. However, some temperatures estimated by Sikes et al.’s (1997) equation from the U_{37}^{K} varied from the observed SST, possibly because of the rapidly changing rate of alkenone synthesis in the logarithmic growth stage or the low rate of alkenone synthesis when nutrients were limiting. Temperatures estimated from U_{37}^{K} in the surface sediments (6.8–8.2°C) matched the observed SST in September (7–8°C) but differed from the annual average SST of 4 to 5°C, suggesting that most of the alkenone in the eastern Bering Sea was synthesized during limited periods, for instance, in September. The relative amounts of $C_{37:4}$ alkenone as proportions of the total alkenones (referred to as $C_{37:4}\%$) were high, ranging from 18.3 to 41.4%. Low-salinity water (<32 psu) within the study area would have contributed to the high $C_{37:4}\%$ because a negative linear relationship between $C_{37:4}\%$ and salinity was found in this study. Copyright © 2003 Elsevier Science Ltd

1. INTRODUCTION

Since it was first realized that alkenones were produced mainly by the haptophyte algae, the coccolithophores *Emiliania huxleyi* and *Gephyrocapsa oceanica* (Volkman et al., 1980; Marlowe et al., 1984a), the alkenone unsaturation indices, U_{37}^{K} and U_{37}^{K} , which are derived from the relative abundance of methyl alkenones with 37 carbon atoms and two, three, or four double bonds, have been proposed as proxy measures of water temperature (Brassell et al., 1986; Prah1 et al., 1988). The U_{37}^{K} index was initially defined as (Brassell et al., 1986)

$$U_{37}^{\text{K}} = (C_{37:2} - C_{37:4}) / (C_{37:2} + C_{37:3} + C_{37:4}).$$

However, $C_{37:4}$ alkenone is often undetected, and so the alkenone unsaturation index was simplified (Prah1 and Wakeham, 1987):

$$U_{37}^{\text{K}} = C_{37:2} / (C_{37:2} + C_{37:3}).$$

Typically, the U_{37}^{K} recorded in surface sediments worldwide exhibits a linear correlation with the average annual sea surface temperature (SST) (Müller et al., 1998), and this “alkenone thermometer” has been accepted as a robust proxy for global and regional reconstruction of the water temperature (Prah1 and Wakeham, 1987; Sikes and Volkman, 1993; Pele-

jero and Grimalt, 1997; Sonzogni et al., 1997; Ternois et al., 1997; Sicre et al., 2002). Besides being extended to reconstructing paleotemperatures (Bard et al., 1997; Pelejero and Grimalt, 1999; Weaver et al., 1999; Goñi et al., 2001; Ishiwatari et al., 2001), alkenones have been used as proxies for estimating the variability of current systems by using the SST profile (Doose et al., 1997) and a biomarker for marine organisms (Ternois et al., 2001). In addition, the $\delta^{13}\text{C}$ of alkenones has been used to estimate the paleo- $p\text{CO}_2$ (Jasper and Hayes 1990; Pagani et al., 1999) and the growth rate of alkenone producers (Bidigare et al., 1997).

However, neither the relationships between alkenone unsaturation and temperature nor those between the $\delta^{13}\text{C}$ of alkenones, growth rate, and $p\text{CO}_2$ can be explained simply (Herbert, 2001). In the northeast Atlantic, U_{37}^{K} in the sediment trap material was anomalously low and showed poor correlation with SST during the spring of 1989 (Rosell-Melé et al., 2000). The discrepancy between U_{37}^{K} and SST means that this relationship might be explained by a calibration that differed from the published ones (Prah1 and Wakeham 1987; Müller et al., 1998). A discrepancy was also found between the U_{37}^{K} in suspended material and the SST (Conte et al., 2001; Sicre et al., 2002).

Although the discrepancies have been attributed to the presence of residual amounts of alkenones in particulate detritus (Conte et al., 1992), to an influx of alkenones from elsewhere (Rosell-Melé et al., 2000), to a retention of alkenones produced

* Author to whom correspondence should be addressed (haradan@jamstec.go.jp).

in the previous season (Sicre et al., 1999), and to environmental influences other than temperature (such as nutrient levels) (Epstein et al., 1998; Popp et al., 1998a; Versteegh et al., 2001), the precise reasons are not clear. Especially under natural conditions on a regional level, present information is insufficient for determining a relationship between alkenone abundance (and its unsaturation pattern) and environmental parameters such as nutrients and salinity (Volkman, 2000).

Flourishes of coccolithophores can be detected by ocean color imagery with data from the satellite-borne Sea-viewing Wide Field-of-view sensor SeaWiEs. Flourishes in the Bering Sea in 2000 were intermittently observable for at least 9 months from the beginning of February to the beginning of November (<http://orbit-net.nesdis.noaa.gov/orad2/doc/ehux.html>). Temporally and spatially large-scale blooms of *E. huxleyi* have occurred annually in the Bering Sea since 1997. In 1997, a combination of atmospheric mechanisms produced summer weather anomalies such as calm winds, clear skies, and warm air temperatures over the eastern Bering Sea, and the weather anomalies caused depletion of the subpycnocline nutrient reservoir (Napp and Hunt, 2001). After depletion of nitrate and silicate, a sustained (more than 4-month-long) bloom of *E. huxleyi* was observed (Stockwell et al., 2001). Because of the speed and magnitude with which parts of the Bering Sea ecosystem responded to changes in atmospheric factors (Napp and Hunt, 2001) and because a bloom of the coccolithophorid *Coccolithus pelagicus* has also been detected in the northeastern Atlantic Ocean off Iceland every year since 1997 (Ostermann, 2001), the appearance of an *E. huxleyi* bloom in the Bering Sea could be related to atmospherically forced decadal oscillations or global factors.

In this study, we were interested in the characteristics of the alkenones produced by the *E. huxleyi* bloom in the Bering Sea in 2000. We discuss the relationship between alkenone content and nutrient levels, as well as the relationship between the $\delta^{13}\text{C}$ of alkenone, $[\text{CO}_2(\text{aq})]$, and bloom stage to clarify the characteristics of alkenones synthesized by a bloom in the eastern Bering Sea. Furthermore, the relationship between the relative content of $\text{C}_{37:4}$ ($\text{C}_{37:4}\%$) alkenone and temperature and salinity is discussed from the viewpoint of using $\text{C}_{37:4}\%$ as a possible indicator of salinity or temperature. As a result, the $\text{C}_{37:4}\%$ is proposed as a proxy of salinity.

2. MATERIALS AND METHODS

Surface water samples were collected in the eastern Bering Sea with a carousel water sampler (Sea-Bird Electronics, Inc., USA), equipped with 24 Niskin bottles and conductivity, temperature, and depth sensors. Sampling was conducted during the MR00-K06 cruise of the R/V *MIRAI* from the beginning of September to the beginning of October 2000 (Table 1 and Fig. 1). Water samples were gravity filtered through glass fiber filters (diameter = 47 mm, effective pore size = $0.7\ \mu\text{m}$) without vacuum on board the *MIRAI*.

The sediment core used in this study was collected at the BR-12 hydrocast station ($63^\circ30'\text{N}$, $165^\circ30'\text{W}$; 35-m water depth) with a multiple core sampler (Rigosha Co., Ltd., Japan). The sediment core was 30 cm long and was cut into 0.5-cm subsamples.

Filter and sediment samples were stored at -20°C until chemical analysis. Filter and sediment samples were freeze dried before extraction. The dried sediment was ground into a powder with an agate mortar and pestle. The bulk organic fractions were extracted from the filter and sediment samples with an accelerated solvent extractor (ASE-200, Dionex Japan, Ltd.) at 100°C and 1000 psi using a mixture of dichloromethane and methanol (99:1 v/v) as the solvent. The yield of

the extraction procedure was $> 95\%$ for a ketone standard (2-nonadecanone).

The extracts were saponified in 0.5-mol/L KOH in methanol at 80°C for 2 h. The neutral fraction was recovered with a pipette, dissolved in hexane, and then separated into subfractions by silica gel column chromatography using an automatic solid preparation system (Rapid Trace SPE Workstation, Zymark, UK). Standards for the subfractionation were hydrocarbons ($\text{C}_{20}\text{--}\text{C}_{38}$ hydrocarbons and 5α -cholestane, GLSciences Inc., Japan), a ketone (2-nonadecanone, Fluka Chemie, Switzerland), and a sterol (cholesterol, GLSciences Inc., Japan). The solvents used were 4 mL of hexane for fraction 1; a mixture of 2 mL of a hexane-toluene mixture (3:1 v/v), 2 mL of hexane-toluene (1:1 v/v), 2 mL of hexane-ethyl acetate (95:5 v/v), and 2 mL of hexane-ethyl acetate (9:1 v/v) for fraction 2; 2 mL of hexane-ethyl acetate (85:15 v/v) followed by 2 mL of hexane-ethyl acetate (4:1 v/v) for fraction 3; and 2 mL of hexane-ethyl acetate (4:1 v/v) followed by 2 mL of ethyl acetate for fraction 4. The alkenones eluted in fraction 3. The recovery of a 2-nonadecanone standard with this procedure was $> 90\%$.

A sample of the alkenone fraction was analyzed by capillary gas chromatography with a Fisons 8000 series gas chromatograph (CE Instruments, USA) equipped with a 50-m-long, 0.32-mm internal diameter Chrompack CP-Sil 5CB fused silica column, a cold on-column injector, and a flame ionization detector. The temperature regime for gas chromatography was as follows: held at 60°C for 1 min, increased to 200°C at $20^\circ\text{C}\ \text{min}^{-1}$, increased to 305°C at $15^\circ\text{C}\ \text{min}^{-1}$, held at 305°C for 32 min, increased to 320°C at $15^\circ\text{C}\ \text{min}^{-1}$, and held at 320°C for 5 min. A hydrocarbon, dotriacontane with deuterium (Cambridge Isotope Laboratories, USA), was used as an internal standard, and we assumed that the flame ionization detector was equally sensitive to C_{37} alkenone and the internal standard.

A major source of error in alkenone analysis is irreversible adsorption onto the chromatographic column. The production rate of $\text{C}_{37:2}$ alkenone in an algal cell is very low at the low temperatures of the Bering Sea; therefore, to reduce error, it was necessary to analyze a relatively large amount of $\text{C}_{37:2}$ alkenone by gas chromatography. We injected the greatest amount possible ($> 100\ \text{ng/injection}$) during each analysis to ensure reliable alkenone quantification. However, for three sediment samples from depths of 7, 11, and 12 cm, the amount of $\text{C}_{37:2}$ alkenone was $< 100\ \text{ng/injection}$, and we were unable to detect alkenone in some samples, in which the amounts of individual $\text{C}_{37:4}$, $\text{C}_{37:3}$, and $\text{C}_{37:2}$ alkenones were $< \sim 10\ \text{ng/injection}$.

$\delta^{13}\text{C}$ analysis was done for $\text{C}_{37:3}$ alkenone in three filter samples (A, B, and C in Table 2) because its concentration was the highest among the three C_{37} alkenones in this study. We used an isotope ratio-monitoring gas chromatograph mass spectrometer system consisting of an HP6890 gas chromatography unit and a Finnigan MAT252 mass spectrometer unit. The $^{13}\text{C}/^{12}\text{C}$ isotopic ratios in an $n\text{-C}_{36}$ hydrocarbon (GLSciences Inc., Japan) and in National Bureau of Standards standard 19 (International Atomic Energy Agency) were also measured as internal standards and as reference materials for the Pee Dee belemnite carbonate, respectively. The replicate errors were ± 0.4 and $\pm 0.5\%$ for $n\text{-C}_{36}$ hydrocarbon and $\text{C}_{37:3}$ alkenone, respectively.

Portions of three filter samples (A, B, and C in Table 1) were also analyzed for total carbon content with a CHN analyzer (2400 Series II, PerkinElmer, USA). The six filter samples (BR-5, BR-6, BR-7, A, B, and C) were exposed to HCl vapor in a desiccator for 0.5 d to remove carbonate. Carbonate-free samples were dried in a desiccator under vacuum and then analyzed for organic carbon content with the CHN analyzer (Table 1). The analytical errors for determination of calcium carbonate and organic carbon by this method were within 7 and 3%, respectively.

3. RESULTS AND DISCUSSION

3.1. Occurrence of *E. Huxleyi* Bloom and Relation Between Levels of Alkenones and Nutrients

The continental shelf of the eastern Bering Sea is one of the most productive areas in the world's oceans (Odate and Saito, 2001). High productivity is maintained by nutrients transported into the euphotic zone by tidal mixing, lateral currents, and

Table 1. Sample locations and content of surface seawater samples from the Bering Sea.

Sample Filter	Lat. N	Long. E	Sampling date	Water volum (l)	Alkenone C ₃₇ content in water (μg/l)			Total C ₃₇ content in water (μg/l)	Total C ₃₇ content in particle (μg/g)	Organic C. content in water (μg/l)	Organic C. content in particle (mg/g)	C _{37:4} in total C ₃₇ (%)	U ₃₇ ^{K'}	NO ₃ μmol/k	SiO ₂ μmol/k	PO ₄ μmol/k	HN ₄ ⁺ μmol/k	Alkenone temp. [†] (°C)	Alkenone temp. ^{††} (°C)	Alkenone temp. ^{†††} (°C)	SST (°C)	SST- alkenone temp.* (°C)	
					C _{37:4}	C _{37:3}	C _{37:2}															SST	temp.*
BR-1	55-00	166-00	1-Sep	6	n.d.*	n.d.	n.d.	-**	-	-	-	-	-	13.4	30.3	1.22	0.5	-	-	-	8.3	-	-
BR-2	55-30	166-00	2-Sep	4	n.d.	n.d.	n.d.	-	-	-	-	-	-	3.81	11.2	0.68	0.7	-	-	-	9.2	-	-
BR-3	56-00	166-00	2-Sep	4	n.d.	n.d.	n.d.	-	-	-	-	-	-	3.76	11.3	0.67	1.1	-	-	-	8.8	-	-
BR-5	57-00	166-00	2-Sep	4	0.110	0.383	0.109	0.603	-	39.0	-	18.3	0.22	3.42	13.2	0.52	0.4	8.0	5.4	5.4	7.6	-0.4	0.00
BR-6	57-30	166-00	2-Sep	3	0.275	0.703	0.234	1.21	-	54.6	-	22.7	0.25	2.43	13.2	0.44	0.9	8.7	6.2	6.2	7.7	-1.0	-0.03
BR-7	58-00	166-00	3-Sep	3	0.578	1.22	0.183	1.98	-	44.6	-	29.2	0.13	0.76	8.50	0.31	1.4	5.6	2.7	2.6	7.0	1.4	-0.20
BR-8	58-30	166-00	3-Sep	4	0.192	0.480	0.096	0.769	-	-	-	25.0	0.17	0.59	8.52	0.47	0.8	6.5	3.8	3.7	7.7	1.2	-0.13
BR-10	62-00	169-00	4-Sep	4	1.29	1.70	0.125	3.12	-	-	-	41.4	0.07	0.12	2.86	0.25	0.1	4.0	0.9	0.7	7.5	3.5	-0.37
BR-12	63-30	165-30	5-Sep	13	n.d.	n.d.	n.d.	-	-	-	-	-	-	5.51	5.51	0.80	1.1	-	-	-	9.6	-	-
A	61-33	168-59	4-Sep	6	0.054	0.101	0.009	0.164	66.4	56.0	33.7	32.7	0.08	-	-	-	-	4.4	1.3	1.2	7.6	3.2	0.36
B	63-05	168-18	1-Oct	6	0.625	0.969	0.126	1.72	349	132	42.1	36.3	0.11	-	-	-	-	5.2	2.2	2.1	5.0	-0.2	0.33
C	59-29	167-26	2-Oct	6	0.045	0.094	0.016	0.155	22.0	162	32.5	29.1	0.14	-	-	-	-	6.0	3.1	3.0	7.9	2.0	0.34

* n.d. = not detected.

** A dash “-” means not determined.

[†] The equation reported in Sikes et al. (1997) was used to convert the alkenone unsaturation index to temperature.

^{††} The equation reported in Prahl et al. (1988) was used to convert the alkenone unsaturation index to temperature.

^{†††} The equation reported in Müller et al. (1998) was used to convert the alkenone unsaturation index to temperature.

The total alkenone content was calculated to be the sum of C_{37:2}, C_{37:3}, and C_{37:4} alkenones contained in 1L units of seawater from each sample.

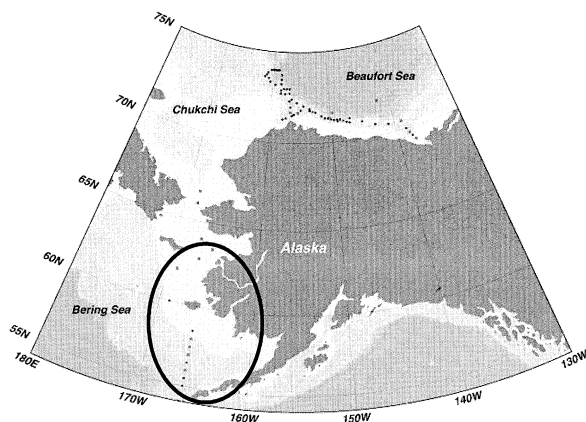


Fig. 1. Locations at which suspended particulates were sampled in the surface water of the eastern Bering Sea. Samples were collected in the area enclosed by the circle. Small dots are the sampling sites.

eddies caused by the Bering Slope current (Springer et al., 1996; Stabeno and Van Meurs, 1999). The $p\text{CO}_2$ values in surface seawater and in air were measured from 54°N to 67°N in the eastern Bering Sea (Fig. 2; Murata and Takizawa, 2002). The $p\text{CO}_2$ value in seawater varied widely with latitude between 220 and 450 μatm . Higher $p\text{CO}_2$ in seawater, 370 to 450 μatm , than in air was observed in the areas from 54°N to 55°N, 57°N to 60°N, 60°N to 62°N, 63°N to 64°N, and 65°30'N to 66°N in the beginning of September and in the areas from 54°N to 55°N, 57°N to 58°30'N, and 59°30'N to 62°N in the end of September and the beginning of October, suggesting that carbonate was actively produced by coccoliths in patchiness of *E. huxleyi* blooms (Murata and Takizawa, 2002). Microscopic observations indicated that the coccolithophorid bloom was composed entirely of *E. huxleyi*, with densities as high as 5×10^6 coccospheres L^{-1} (H. Okada, personal communication), corresponding to a density of 4.5×10^6 coccospheres L^{-1} in the 1997 bloom (Stockwell et al., 2001).

Twelve samples of suspended particulates collected from 55°N to 63°N in the eastern Bering Sea were used for analysis of $\text{C}_{37:2}$, $\text{C}_{37:3}$, and $\text{C}_{37:4}$ alkenones (Table 1; Fig. 1). In September, alkenone was detected only between 57°N and 62°N (Table 1; Fig. 3). The alkenone concentrations were below the limits of detection near the boundaries between the Bering Sea and the Chukchi Sea and between the Bering Sea and the North Pacific, although alkenone was detected at 63°N near the boundary between the Bering Sea and the Chukchi Sea in October. This finding suggests that the bloom area was limited to 57°N to 63°N and nearly corresponded to the areas of high $p\text{CO}_2$ in seawater (Fig. 2) during September and Oc-

tober 2000. In the area from 54°N to 55°N, alkenone was not detected, although $p\text{CO}_2$ in the surface seawater was high, 450 μatm .

We compared the appearance of alkenones with the contour profiles of the concentrations of phosphate, silicate, nitrate, and ammonium (Sato et al., 2001) above the continental shelf of the Bering Sea (Fig. 4a). These nutrient data were collected at the beginning of September 2000. In the 55°N to 60°N area, the surface water concentrations of all nutrients were low, but phosphate, silicate, and nitrate increased with depth and proximity to the Pacific Ocean, suggesting that water masses with relatively high nutrient concentrations were laterally advected from the Pacific to the Bering Sea. Conversely, concentrations of ammonium at depths of ~50 to 60 m were very high near the edge of Bering Shelf. These high concentrations of ammonium might have come from degraded material that settled from the surface bloom.

The high-ammonium water mass formed a dome around the Bering Shelf, and the vertical temperature profile also dropped within this water mass (Fig. 4b). The eastern coast of the Bering Sea is covered with sea ice in winter and is influenced by Alaskan coastal water (including runoff from the Yukon River). The combination of wind mixing and melting ice can cool the water column to near the freezing point of seawater. As the sea surface warms during the spring and summer, this isolates the cold bottom water, resulting in a feature known as the cold water mass. The temperature of the upper mixed layer and its thickness over the cold water mass depend on the strength and timing of storms and on the thermodynamic balance between heat content from the previous summer and extent of sea ice in the winter (Stabeno et al., 2001). In 1997, unusual physical conditions occurred in the eastern Bering Sea: strong May storms and calm conditions in July, which brought high SST, a shallow wind-mixed layer, a fresher than normal water column, and unusual cross-shelf currents (Stabeno et al., 2001). Accompanying these conditions were changes in the dominant phytoplankton, including significant new productivity below the shallow pycnocline in the spring, which depleted the subpycnocline nutrient reservoir and was followed by a bloom of *E. huxleyi* for > 4 months in 1997 (Napp and Hunt, 2001). Similar unusual physical conditions might have resulted in the bloom during September and October 2000, too.

Mizobata et al. (2001) observed the occurrence of an eddy in the eastern Bering Sea in 2000 centered at 55°30'N, 171°W, with high concentrations of chlorophyll *a* at the margin of the eddy, indicating a bloom of *E. huxleyi*. Wind strength is also considered important for the occurrence of *E. huxleyi* blooms. Iida and Saito (2001) observed coccolithophorid blooms in 1997, 1998, and 1999 and noted that extensive blooms occurred

Table 2. Elemental analysis and ratio of stable carbon isotopes in alkenone in suspended particles; salinity and $p\text{CO}_2$ in the surrounding.

MR00-K06 Filter	Salinity	$p\text{CO}_2$ (μatm)	Total C. (%)	Inorganic C. (%)	Organic C. (%)	C/N mol ratio	Co/Ci	alkenone $\delta^{13}\text{C}$ (‰ PDB)	b-value* (‰ μmol)
A	30.617	385.8	7.83	4.46	3.37	7.1	0.76	-26.3	132
B	31.520	330.6	5.99	1.79	4.21	7.7	2.36	-29.7	86
C	31.519	425.9	10.5	7.21	3.25	7.7	0.45	-27.0	135

* The b-value is a parameter of the growth rate of phytoplankton and reflects the intracellular carbon demand.

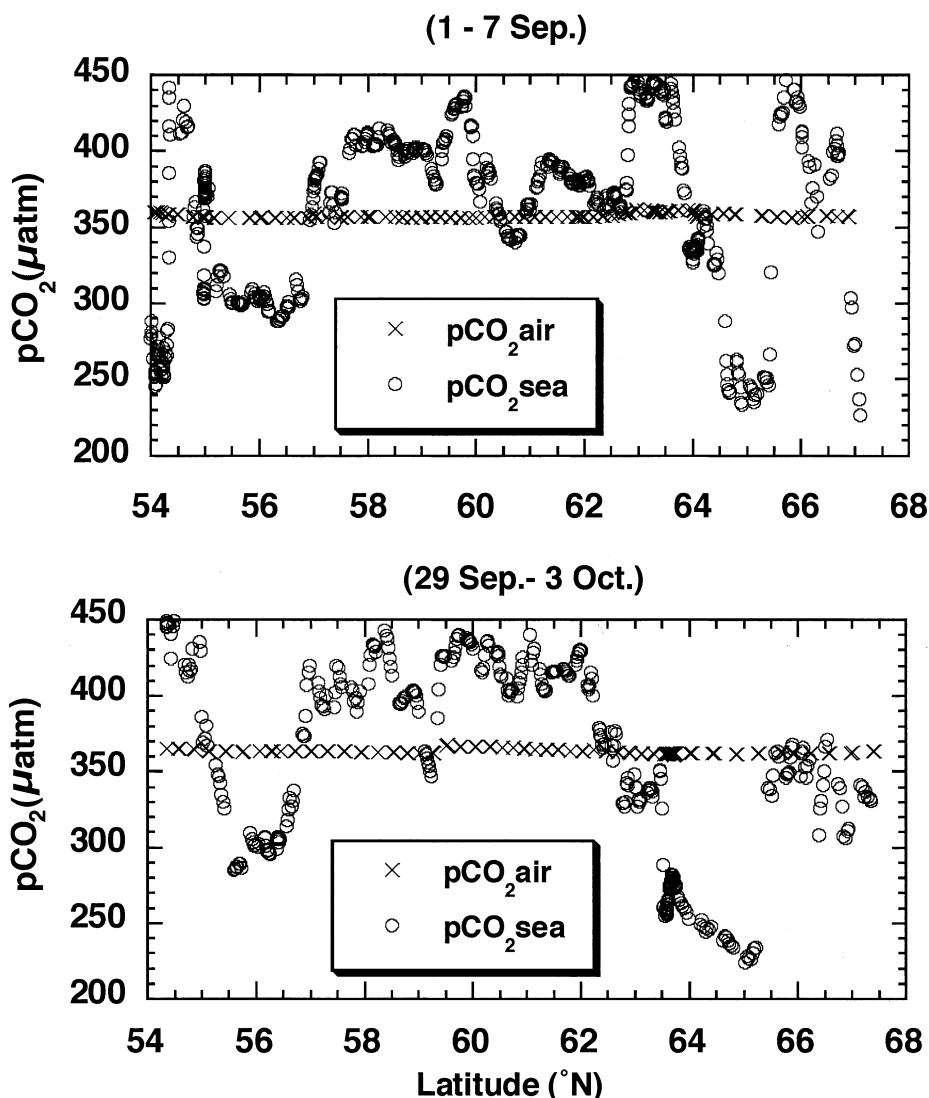


Fig. 2. Continuous measurement of $p\text{CO}_2$ in the surface seawater and in the air from 54°N to 67°N in the eastern Bering Sea. Reproduced with permission from Murata and Takizawa (2002).

under calm wind conditions when the surface water was stable and stratified. Therefore, the presence of an extensive bloom in September and October 2000 in the eastern Bering Sea might also have been facilitated by eddy development and calm winds. Although the mechanism maintaining the sustained bloom is still unknown, a large stable cold water mass having a high ammonium concentration might function as a nutrient reservoir for surface water blooms of *E. huxleyi* (Shin et al., 2002).

Alkenones were detected where the nitrate, silicate, and phosphate concentrations were low and the ammonium/nitrate ratios relatively high (Fig. 4a, Table 1). A similar relationship between the appearance of alkenone producers and phosphate was found in mesocosm observations in the Norwegian fjords (Egge and Heimdahl, 1994) and in computer simulations (Aksnes et al., 1994). Another study that modeled blooms of *E. huxleyi* in the northeast Atlantic showed that blooms occurred when the parameters were adjusted to show adaptation of *E.*

huxleyi to low phosphate concentration and high light intensity (Nanninga and Tyrrell, 1996; Tyrrell and Taylor, 1996). In addition, observations of a natural bloom of *E. huxleyi* indicated that the bloom was regulated by low phosphate (Townsend et al., 1994). Multispecies chemostat experiments have obtained greater numbers of *E. huxleyi* at high nitrate/phosphate ratios (Riegman et al., 1992).

3.2. The Contents of Alkenone and Organic Carbon in Suspended Particles and Sediments

The total C_{37} alkenone content of suspended particles in the water showed high variability, between 0.155 and $3.12 \mu\text{g L}^{-1}$ (Table 1). This large difference in alkenone content among the sampling stations indicates different population densities of *E. huxleyi* in the eastern Bering Sea. These values were one tenth those observed during the later stages of a bloom and in the postbloom period of an *E. huxleyi* bloom in Samnangerfjorden

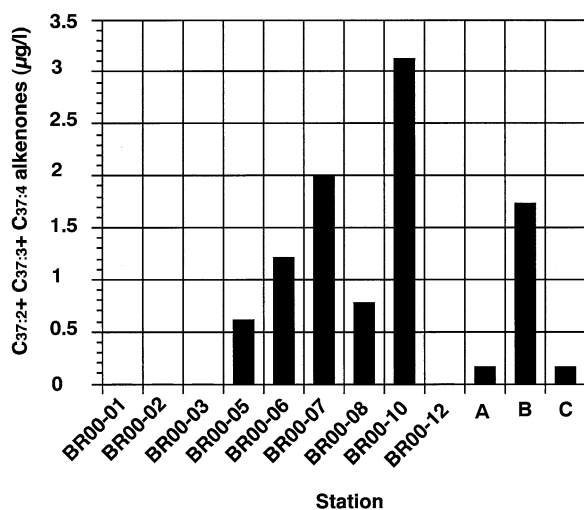


Fig. 3. Total alkenone ($C_{37:2}$, $C_{37:3}$, and $C_{37:4}$) concentration ($\mu\text{g L}^{-1}$ of seawater) in suspended particulate samples from the surface water of the eastern Bering Sea. No alkenones were detected in the blank column.

(Conte et al., 1994a). The total C_{37} alkenone contents in our study were 10 to 100 times the levels found in suspended particles collected under nonbloom conditions in the surface waters of the North Atlantic and Nordic Sea (Sicre et al., 2002) and in the western Sargasso Sea (Conte et al., 2001).

For three filter samples, A, B, and C, alkenone content per gram of suspended particle ranged from 22.0 to 349 $\mu\text{g g}^{-1}$ dry weight (Table 1), with a mean of 146 $\mu\text{g g}^{-1}$. The organic carbon content in the suspended particulate samples ranged from 32.5 to 42.1 mg g^{-1} (Table 1). Previous studies with controlled cultures found that the alkenone contents of cells of *E. huxleyi* changed with growth stage, accounting for up to 8 to 15% of the organic matter in cells in late stages (Prahl et al., 1988; Epstein et al., 1998). The total C_{37} alkenone contents in our study were 0.03 to 0.4% of the organic matter (which is assumed to be about twice the organic carbon content) in the suspended particles and extremely low compared with the results from these culture experiments. This suggests that the cells were in a more stressed condition in the field and, accordingly, produced less alkenone. Furthermore, although almost all microscopically visible particles in water samples were cells of *E. huxleyi*, most of the organic matter of the suspended particles in the water on the continental shelf of the eastern Bering Sea was from other sources.

The C_{37} alkenone content per gram (dry weight) of the surface sediment decreased with depth from 1.42 $\mu\text{g g}^{-1}$ at the sediment surface to 0.109 $\mu\text{g g}^{-1}$ at 11 cm depth and was not detected at depths of > 13 cm (Table 3). The C_{37} alkenone content we found was one tenth to one hundredth of what was measured in the sediment in the Santa Monica Basin (Gong and Hollander, 1999) and in the Guaymas Basin, Gulf of California (Goñi et al., 2001), which are both beneath low-oxygen water columns, and was almost the same as or half the level in surface sediments collected in the Sea of Japan (Ishiwatari et al., 2001). The C_{37} alkenone content in our study was 10 to 100 times that in Okhotsk Sea sediment (Ternois et al., 2001), perhaps because the Bering Sea is shallower than the Okhotsk Sea. During

the bloom or postbloom periods in the eastern North Atlantic, the alkenone produced in the surface water immediately decomposed, and the concentration decreased 10-fold to 100-fold at depths below the seasonal thermocline (Conte et al., 1992). Gong and Hollander (1999) reported that a drastic decomposition of alkenone occurred within a few centimeters below the top of the sediment, and the alkenone content in the surface layer of oxic sediments was only one third that in anoxic sediments. The dissolved oxygen concentration in the bottom water was > 250 $\mu\text{mol kg}^{-1}$ at each of our study sites (Komai and Wataki, 2000), and thus, the sediment surface was oxic. The alkenone content at the sediment surface was < 1% of the concentration in suspended particles in the surface water. This implies that most of the particulate alkenones produced in the surface water were rapidly degraded in the water column or at the interface between water and sediment before accumulating in the sediment, despite the relatively shallow depth (70 m) of the continental shelf of the Bering Sea. Bacterial biomass and activity are generally higher in the central Bering Sea (Nagata et al., 2001); thus, bacterial activity may be responsible for the large difference between alkenone concentrations in the surface water and at the sediment surface.

According to Younker et al. (1995), on the Mackenzie Shelf of the Arctic Ocean, terrigenous particle input is large, and most hydrocarbons are of terrigenous origin. In the continental shelf area, large amounts of terrigenous materials, not only organic materials but also clay minerals, are added to autochthonous organic materials, which dilute the marine-produced organic content of that sediment. A similar dilution effect could also contribute to the low alkenone content in the surface sediment compared with that in the water column.

3.3. Difference of Bloom Status of *E. Huxleyi* Among Sampling Stations

The ratios of stable carbon isotopes in organic materials produced by marine organisms are affected by many environmental factors, such as fluctuations in dissolved CO_2 (Jasper and Hayes, 1990; François et al., 1993; Bentaleb et al., 1996). In addition, when organic materials are produced by marine phytoplankton, the carbon isotope composition is influenced by the growth rate (Bidigare et al., 1997), cell leakiness (Badger et al., 1985), cell geometry (Popp et al., 1998b), species (Rau et al., 1997), and irradiance (Johnston, 1996) at each stage of the bloom. For alkenones, the ratio of stable carbon isotopes is affected mainly by the growth rate of the alkenone producer (Bidigare et al., 1997; Popp et al., 1998a) and the concentration and isotopic composition of the dissolved CO_2 (Jasper et al., 1994). When the growth rate of the alkenone producer is high, the ratio of stable carbon isotopes in $C_{37:2}$ alkenone (referred to as $\delta^{13}\text{C}$ alkenone) becomes heavy, that is, the alkenone is enriched in ^{13}C (Andersen et al., 1999; Riebesell et al., 2000b). When the concentration of dissolved CO_2 is high, the alkenone becomes depleted in ^{13}C (isotopically light) (Andersen et al., 1999; Riebesell et al., 2000b). In our study, we wanted to clarify which factor, *E. huxleyi* growth rate or dissolved CO_2 concentration, mainly affected the $\delta^{13}\text{C}$ of alkenone. Because we determined the $\delta^{13}\text{C}$ for only $C_{37:3}$ alkenone, we therefore need to assume that $\delta^{13}\text{C}_{37:3}$ alkenone is directly proportional to $\delta^{13}\text{C}_{37:2}$ alkenone to relate our results to those of others.

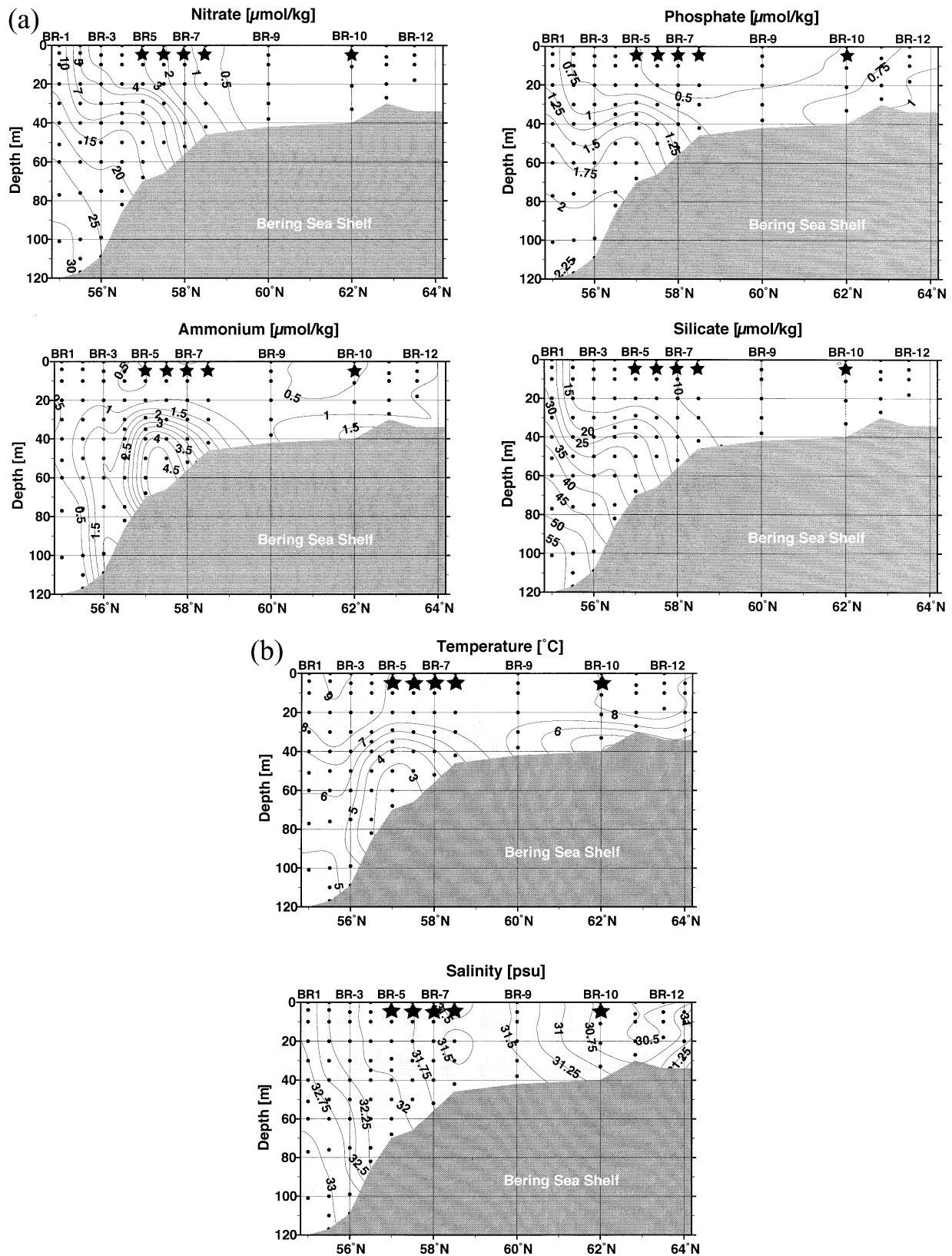


Fig. 4. Vertical profiles of (a) nitrate, ammonium, phosphate, and silicate and (b) temperature and salinity in the eastern Bering Sea in September 2000. The stars indicate sites where alkenone was detected in the September observations.

Table 3. Alkenone contents of sediment sample collected at station BR-12 in the Bering Sea.

Depth (cm)	Dry weight (g)	Alkenone content ($\mu\text{g/g}$)			$C_{37:2} + C_{37:3}$ content ($\mu\text{g/g}$)	$C_{37:4}$ in total C_{37} (%)	$U_{37}^{\text{K}'}$	Alkenone temp* ($^{\circ}\text{C}$)
		$C_{37:4}$	$C_{37:3}$	$C_{37:2}$				
1	9.55	0.508	0.729	0.183	1.42 ($C_{37:2} + C_{37:3} + C_{37:4}$)	35.8	0.20	7.4
3	9.54	–	0.478	0.102	0.580	–	0.18	6.8
4	9.17	–	0.440	0.107	0.547	–	0.20	7.3
5	9.49	–	0.525	0.122	0.647	–	0.19	7.1
7	10.3	–	0.197	0.045	0.243	–	0.19	7.1
9	9.48	–	0.289	0.071	0.360	–	0.20	7.3
10	9.76	–	0.158	0.036	0.194	–	0.19	7.1
11	9.68	–	0.084	0.025	0.109	–	0.23	8.2
13	9.83	n.d.	n.d.	n.d.	–	–	–	–

* The equation reported in Sikes et al. (1997) was used as to convert the alkenone index to temperature.

** n.d. = not detected.

*** A dash “–” means not calculated, because the subsamples of the sediment core from 3 to 11 cm depth had a slight shoulder on the $C_{37:4}$.

We found $\delta^{13}\text{C}_{37:3}$ alkenone values of -26.3 , -29.7 , and -27.0‰ at locations A, B, and C, respectively. The $\delta^{13}\text{C}_{37:3}$ alkenone was clearly higher at locations A and C than at location B (Table 3), suggesting that either the concentration of dissolved CO_2 in the water may have been lower at collection points A and C than at B or that the growth rate of *E. huxleyi* was higher at A and C than at B. However, the concentration of dissolved CO_2 , $[\text{CO}_2(\text{aq})]$, converted by pCO_2 ($\text{pCO}_2 \approx \text{PCO}_2$ at 100% humidity) via Henry's law using the in situ temperature and salinity (Tables 1 and 2), was higher at A and C than at B. Thus, differences in dissolved CO_2 cannot explain our results. Furthermore, Riebesell et al. (2000b) estimated the effects of varying CO_2 concentration on the carbon isotope fractionation of alkenone in *E. huxleyi* in culture and found that the carbon isotope fractionation of $C_{37:3}$ alkenone associated with the same $[\text{CO}_2(\text{aq})]$ as at our stations B ($\sim 17 \mu\text{mol kg}^{-1}$) and C ($\sim 20 \mu\text{mol kg}^{-1}$) was $< 1\text{‰}$. The difference of $\delta^{13}\text{C}_{37:3}$ alkenone between samples B and C is $\sim 3\text{‰}$ and cannot be explained by the change in $[\text{CO}_2(\text{aq})]$. Therefore, we infer that the $\delta^{13}\text{C}$ alkenone was mainly affected by the growth rate of the *E. huxleyi* rather than by the $[\text{CO}_2(\text{aq})]$.

We therefore estimated the growth rate of *E. huxleyi* for samples A, B, and C as the b value ($\text{‰}\mu\text{mol}$, Eqn. 1), which reflects the intracellular carbon demand. According to Bidigare et al. (1997), the b value is closely and positively correlated with the growth rate of phytoplankton. The equation is expressed as

$$b = (\varepsilon_f - \varepsilon_p) \times [\text{CO}_2(\text{aq})]. \quad (1)$$

To calculate the b value using Eqn. 1, we need the concentration, $[\text{CO}_2(\text{aq})]$; the isotopic fractionation accompanying photosynthetic carbon fixation, ε_p ; and the combined fractionation of carbon isotope due to the enzymes rubisco and β -carboxylase for *E. huxleyi*, ε_f (Andersen et al., 1999). The $[\text{CO}_2(\text{aq})]$ can be calculated by Henry's law from the pCO_2 in oceanic waters and the CO_2 solubility coefficient, α :

$$\text{pCO}_2 = [\text{CO}_2(\text{aq})]/\alpha. \quad (2)$$

For the ε_f value, we used 25‰ , which has been reported for a marine alkenone producer (Bidigare et al., 1997). The ε_p value is generally described by this equation:

$$\varepsilon_p = [(\delta d + 1000)/(\delta p + 1000) - 1] \times 1000, \quad (3)$$

where δd is the isotopic composition of carbon in $\text{CO}_2(\text{aq})$, and δp is the isotopic composition of carbon in the products of photosynthesis. Because we did not measure the δd , we calculated δd with this equation (Mook et al., 1974):

$$\begin{aligned} \varepsilon b(a) &= [(\delta d + 1000)/(\delta b + 1000) - 1] \times 1000 \\ &= 24.12 - 9866/T, \end{aligned} \quad (4)$$

where $\varepsilon b(a)$ is the temperature-dependent carbon isotope fractionation of $\text{CO}_2(\text{aq})$ with respect to HCO_3^- , δb is the isotopic composition of total dissolved CO_2 , and T is the temperature (K). We did not measure δb either; therefore, the reference value for sea surface water, $+2.2\text{‰}$ (Craig, 1970), was used. Also, δp was estimated by using a constant isotopic fractionation, $\varepsilon_{\text{alkenone}} = 4.2\text{‰}$ (Popp et al., 1998a). $\varepsilon_{\text{alkenone}}$ is nearly equal to $\Delta\delta = \delta p - \delta^{13}\text{C}_{37:2}$ alkenone (Andersen et al., 1999). The b values at A and C were ~ 1.6 times the b value at B (Table 2). This indicates that the growth rates of *E. huxleyi* at locations A and C were indeed much higher than at B.

The ratios of organic to inorganic carbon (C_o/C_i) at A and C were 0.76 and 0.45, respectively, and smaller than at B, where it was 2.36 (Table 2). Hence, *E. huxleyi* located at A and C calcified in preference to fixing carbon into organic matter, resulting in higher pCO_2 values in the water at these sites than at B. This suggests that *E. huxleyi* aggressively releases CO_2 during active growth but fixes carbon into organic matter more than it produces calcium carbonate when growth rates slow. The high alkenone and organic carbon contents in the water samples from site B relative to those at A and C (Table 1) further support this interpretation. Results from our study indicate that natural blooms of *E. huxleyi* may restrict calcification and shift their production toward organic carbon when pCO_2 in the water is higher (Table 2). Experiments with *E. huxleyi* in culture also showed that organic carbon and carbonate production are strongly affected by the CO_2 concentration: higher pCO_2 in the water results in lower ratios of inorganic to organic carbon (calcite C/organic C) (Riebesell et al., 2000a).

3.4. Alkenones as a Measure of Temperature

An alkenone unsaturation index was determined for our filter and sediment samples and used to calculate the temperature, using three equations from the literature. The calculated temperatures were then compared with the actual temperatures.

1. $T = (U_{37}^K + 0.082)/0.038$, obtained from the relationship between the alkenone index, U_{37}^K , of top core samples and SST values of 4 to 17°C in the Southern Ocean (Sikes et al., 1997).
2. $T = (U_{37}^K - 0.039)/0.034$, obtained from cultures of *E. huxleyi* and SST values of 8 to 25°C (Prahl et al., 1988).
3. $T = (U_{37}^K - 0.044)/0.033$, based on alkenones in worldwide surface sediments and confirmed by its general applicability over a temperature range of 0 to 28°C (Müller et al., 1998).

The SST observed at each sampling station in the eastern Bering Sea during our study was 5.0 to 9.6°C (Table 1). The alkenone temperature estimated by Sikes et al.'s (1997) equation was 4.0 to 8.7°C and generally corresponded to the observed SST (Table 1), although large differences occurred between the alkenone-calculated and observed SSTs at stations BR-10, A, and C. The alkenone temperatures calculated with Prahl et al.'s (1988) and Müller et al.'s (1998) equations were similar and ranged from 0.7 to 6.2°C. The discrepancies between the alkenone temperatures calculated with Prahl et al.'s (1988) and Müller et al.'s (1998) equations and the observed SSTs were relatively large.

We mentioned the possibility of rapid microbial degradation of organic materials such as alkenones produced by the bloom. A study by Teece et al. (1998) of the effects of bacterial diagenesis on lipids in *E. huxleyi* found that extensive degradation of C_{37} methyl alkenones occurred under both oxic and anoxic conditions. However, the U_{37}^K index remained essentially constant, except for a slight increase ~750 d after alkenone was synthesized. Therefore, we consider that the effect of bacterial degradation of alkenones on U_{37}^K can also be ignored in our study.

In other studies, the temperature calculated from U_{37}^K (in suspended particles) with Prahl et al.'s (1988) equation was much closer to the observed temperature (Herbert, 2001). We feel that the divergence from Prahl et al.'s (1988) and Müller et al.'s (1998) equations in the Bering Sea is due to some unknown factors, which can be ignored in the general calibration that affects U_{37}^K . Sikes et al.'s (1997) equation was calibrated in the Southern Ocean, which is characterized by low temperatures, low salinity, and high contents of $C_{37:4}$ alkenone (referred to as the 37:4%) in particulate matter. According to the alkenone data in core-top sediments from Nordic seas (Rosell-Melé, 1998), the 37:4% increases strongly at SSTs colder than 5.5 to 6°C, and when the 37:4% is higher than 5%, the scatter in U_{37}^K values increases. This pattern also occurs in the Southern Ocean (Sikes et al., 1997). Our study showed that the greatest difference between U_{37}^K and SST was found at BR-10, which had a high 37:4%, 40%. The reason that the relationships between U_{37}^K in suspended particulate organic carbon and the actual temperature in the Bering Sea agreed better with Sikes et al.'s (1997) equation could be interregional similarities between the Southern Ocean and the Bering Sea, such

as low salinity and relatively high 37:4% values, compared with the open ocean. The Bering Sea also has relatively low salinity (30–32 psu) compared with the open ocean. Sonzogni et al. (1997) reported on the effect of salinity on alkenone ratios in the northern Indian Ocean, where the surface water exhibits a large salinity gradient from the Arabian Sea (annual mean > 36 psu) to the Bay of Bengal (annual mean < 32 psu). They carried out statistical calculations that included salinity in the U_{37}^K -SST regression, attempting to improve the relationship between temperature calculated from U_{37}^K and the observed SST. The inclusion of salinity in the U_{37}^K -SST regression, however, did not result in higher correlation coefficients, and there was no clear influence of salinity (<32 psu) on the U_{37}^K -SST regression. In the Nordic seas, the alkenone in the core-top sediment yielded relatively scattered U_{37}^K values, corresponding to those produced under low salinity (<33 psu) (Rosell-Melé, 1998). Alkenones appear to function as metabolic storage products rather than as membrane molecules (Epstein et al., 2001). Therefore, low salinity could lead to metabolic stress in alkenone producers and thus could cause an irregular relationship between U_{37}^K and SST.

Culture experiments with *E. huxleyi* and *G. oceanica* indicated that nutrient limitation affects the U_{37}^K (Conte et al., 1995; Epstein et al., 1998; Popp et al., 1998a). Culture experiments with another alkenone producer, *Isochrysis galbana*, showed that U_{37}^K values decrease (equivalent to a temperature decrease of ~6°C) when light or phosphate level limits algal growth, but nitrogen limitation appears to have no effect (Versteegh et al., 2001). Because particulate samples were collected from surface water, the effect of light limitation on U_{37}^K can be ignored in our study. The difference between the alkenone-calculated temperature and the observed SST was relatively larger at lower nutrient (nitrate and phosphate) concentrations, and U_{37}^K was also lower at lower nutrient concentrations (Table 1). Epstein et al. (2001) reported that alkenones in *E. huxleyi* were used as metabolic storage components in cells, but the U_{37}^K changed only slightly even when the alkenone concentration in cells decreased due to metabolic utilization in dark batch culture.

Epstein et al. (1998) reported that the ratio of unsaturated alkenones produced during the logarithmic growth phase of cultured *E. huxleyi* was unstable, and the calculated alkenone temperature was far from the actual temperature. However, during the stable growth period, the alkenone-calculated temperature was close to the actual temperature (Epstein et al., 1998). Our results indicated higher growth rates at stations A and C than at B (Table 2). Thus, the results from this natural bloom of *E. huxleyi* support the finding that large differences between the alkenone-calculated temperature and the observed SST occur when *E. huxleyi* is in the rapid growth phase. Then, when the bloom stabilized, such as at B, the alkenone-calculated temperature was close to the measured temperature.

The alkenone temperature of the surface sediment, calculated by using Sikes et al.'s (1997) equation, ranged from 6.8 to 8.2°C (Table 3), and its vertical variability was within 1.5°C. Because the alkenone-calculated temperature recorded in the sediment represents an integrated value on a scale of months (at least) to years, the results are averaged values. The alkenone-calculated temperature corresponded to the in situ SST in September (7–8°C; U.S. National Oceanographic Data Center,

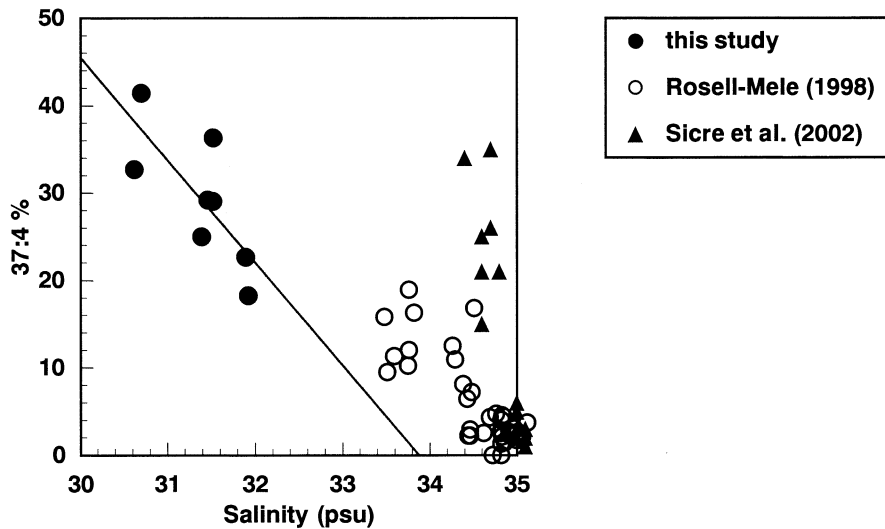


Fig. 5. Relationship between the relative amount of $C_{37:4}$ in total alkenones of suspended particulate samples and local salinity. Black circles indicate data analyzed in this study, open circles are from Rosell-Melé (1998), and solid triangles are from Sicre et al. (2002).

1998). Because there are no whole-year data for alkenone production, the main season of alkenone production in the eastern Bering Sea cannot be determined yet. However, the average annual SST in the study area is 4 to 5°C (U.S. National Oceanographic Data Center, 1998), suggesting that the alkenone-calculated temperature in the sediment may be more closely related to the SST during the main period of algal growth than to the annual average SST.

3.5. Relationships Between $C_{37:4}$ % and Salinity, Temperature, and Nutrients

Although the presence of $C_{37:4}$ alkenone in natural and cultured *E. huxleyi* samples has been reported (Marlowe et al., 1984b; Brassell et al., 1986), its significance is not clear. $C_{37:4}$ alkenone has been observed mainly in high-latitude waters (e.g., Sikes et al., 1997; Rosell-Melé, 1998; Bendle and Rosell-Melé, 2001; Sicre et al., 2002) and low-salinity environments, including lakes (e.g., Li et al., 1996). As reported previously, $C_{37:4}$ alkenone levels become relatively high in colder waters such as those of the Southern Ocean (40% in the sediment at 3.8°C; Sikes et al., 1997), the Nordic seas (19% in the sediment at 3.2°C; Rosell-Melé, 1998), and the North Atlantic, including the Nordic seas (35% at 4.6°C in the water column; Sicre et al., 2002). The $C_{37:4}$ alkenone content in suspended particulate samples was extremely high in our study: the $C_{37:4}$ % ranged from 18.3 to 41.4% (Table 1); however, relatively high values of $C_{37:4}$ have been found by others also (Marlowe et al., 1984b; Freeman and Wakeham, 1992; Conte et al., 1994b; Sikes et al., 1997; Rosell-Melé, 1998; Ohkouchi et al., 1999; Sicre et al., 2002). A common feature among areas in which $C_{37:4}$ is detectable is that they have freshwater inflows, such as from rivers, low-salinity currents, or sea ice. Temperature and salinity data indicate that the water mass at our study site was composed mainly of North Pacific water and Yukon River water (Tanaka et al., 2001). The salinity of the eastern Bering Sea surface water was < 32 psu, and autumn temperatures were

7 to 8°C. We plotted $C_{37:4}$ % against the local salinity at the surface along with previous data obtained from the Nordic seas (Rosell-Melé, 1998; Sicre et al., 2002) (Fig. 5). Regarding our data, the linear negative relationship between $C_{37:4}$ % and salinity (S , in psu) can be described by the equation $C_{37:4} \% = 397.6 - 11.7S$, $r = 0.76$, $n = 8$. Although $C_{37:4}$ % has been suggested as a good indicator of salinity (Rosell-Melé, 1998; Sicre et al., 2002), the relationship between $C_{37:4}$ % and salinity does not appear to be the same in the different study areas. The previous studies also reported a correlation between $C_{37:4}$ % and SST (Rosell-Melé 1998; Bendle and Rosell-Melé, 2001). In contrast, as in the Southern Ocean, we found no relationship between $C_{37:4}$ % and temperature in our study (Fig. 6). This implies that $C_{37:4}$ alkenone production might be regulated by

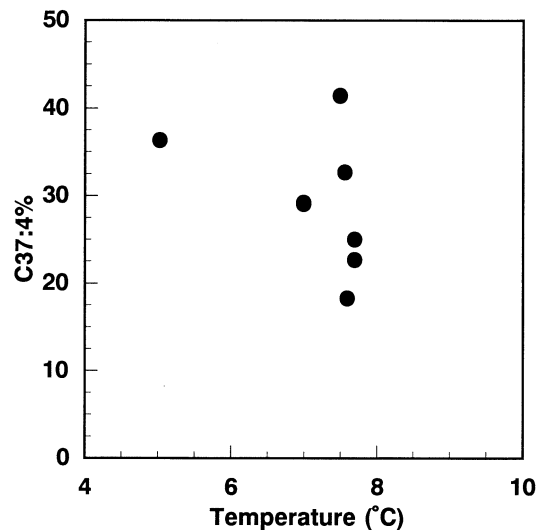


Fig. 6. Relationship between the relative amount of $C_{37:4}$ in total alkenones of suspended particulate samples and local temperatures.

changes in salinity more than by temperature and that low salinity might impose stress on the production mechanism of alkenones and accelerate $C_{37:4}$ production in the Bering Sea.

The slope and y-intercept determined in this study (Fig. 5) differed from those reported by Rosell-Melé (1998), $C_{37:4}\% = 304.95 - 8.66S$, and by Sicre et al. (2002), $C_{37:4}\% = 1691 - 48.1S$. Our study concerned short-term data from one *E. huxleyi* bloom in the Bering Sea, but Rosell-Melé's (1998) study used temporally integrated data from surface sediments in the Nordic seas. However, Sicre et al.'s (2002) relationship was also based on particles in the water. Culture experiments of *E. huxleyi* indicate that $C_{37:4}\%$ is strongly strain dependent (Conte et al., 1995), and this may account for some of the variation in the equations.

The $C_{37:4}\%$ was higher at the northern BR-5 stations (Table 1), but the nitrate and phosphate concentrations were lower at these higher latitude stations, suggesting a negative relationship between $C_{37:4}\%$ and nitrate and phosphate. However, $C_{37:4}\%$ correlates positively with the ammonium/nitrate ratio, except at BR-10 (Table 1). Because only five snapshot data points were available to explain the relationship between $C_{37:4}\%$ and nutrients in this study, more investigations are needed to clarify whether a correlation exists between $C_{37:4}\%$ and nutrients.

4. SUMMARY

We investigated the characteristics of alkenones produced by an *E. huxleyi* bloom in the Bering Sea from the beginning of September to the beginning of October 2000. The main findings are as follows:

1. On the basis of alkenones detected in particulate samples, the bloom patches were limited to an area from 57°N to 63°N, where there was high pCO_2 in the seawater, low nitrate and phosphate concentrations, and high ammonium/nitrate ratios in the surface water.
2. The total alkenone content per gram of suspended particles was between 22.0 and 349 $\mu g g^{-1}$ dry weight. These values accounted for only 0.03 to 0.4% of the total organic matter, suggesting that alkenone was a minor part of the total organic matter in the eastern Bering Sea, despite the extensive *E. huxleyi* bloom. The total alkenone content per gram of sediment sample generally decreased with depth and was < 1% of the total alkenones of the suspended particles in the water. A large proportion of the particulate alkenones synthesized in the surface water was apparently rapidly degraded as the particles settled down the water column.
3. For three particulate samples taken at stations A, B, and C, the carbon isotope ratios ($\delta^{13}C_{37:3}$) in alkenone were -26.3, -29.7, and -27.0‰, respectively. The difference in $\delta^{13}C_{37:3}$ alkenone among the samples could not be explained by changes in $[CO_2(aq)]$ but strongly depended on the growth rate of *E. huxleyi*. On the basis of the $\delta^{13}C_{37:3}$ alkenone values, growth rates of *E. huxleyi* were estimated for each site as the intracellular carbon demand (b value), and the growth rate of *E. huxleyi* at A and C was ~1.6 times that at B.
4. The U^{K}_{37} index was converted to a measure of temperature with three different equations (Prahl et al., 1988; Sikes et al., 1997; Müller et al., 1998). Sikes et al.'s (1997) equation generally gave the best correspondence to the observed

SSTs from the alkenone unsaturation index values in the eastern Bering Sea. However, some samples showed high discrepancies between the alkenone-calculated and the observed temperatures. This difference might be caused by stress due to nutrient limitation and to differences in growth status; as a result, alkenone synthesis could be variable. Conversely, the temperature calculated from alkenones in the surface sediment, which represents values integrated over a time scale of at least months to years, ranged from 6.8 to 8.2°C, corresponding to the SST in September (7–8°C), and was different from the annual average SST (4–5°C). This suggests that a large proportion of alkenone is mainly produced in limited periods, such as September, in the eastern Bering Sea.

5. The relative amounts of $C_{37:4}$ in total alkenones were high, ranging from 18.3 to 41.4%. The surface water salinities in this study area were low, and high $C_{37:4}\%$ values are common in such areas. The relationship between $C_{37:4}\%$ and salinity was linear, suggesting that $C_{37:4}\%$ in the sediment may be an indicator of salinity (Rosell-Melé, 1998; Sicre et al., 2002).

Acknowledgments—We are grateful to Captain Hashimoto and the rest of the crew and scientists of the R/V *MIRAI* for their help in collecting the water samples. We thank our chief scientist on this cruise, Dr. T. Takizawa, and the group leader of the Observational Frontier Research System for Global Climate Change/International Arctic Research Center, Dr. N. Tanaka, for their support of all aspects of this study. Thanks are also due to anonymous reviewers of the manuscript for their comments and suggestions for improvements.

Associate editor: R. Summons

REFERENCES

- Aksnes D. L., Egge J. K., Rosland R., and Heimdal B. R. (1994) Representation of *Emiliania huxleyi* in phytoplankton simulation models: A first approach. *Sarsia* **79**, 291–300.
- Andersen N., Müller P. J., Kirst G., and Schneider R. R. (1999) Alkenone $\delta^{13}C$ as a proxy for past pCO_2 in surface waters: Results from the late Quaternary Angola current. In *Use of Proxies in Paleoceanography: Examples From the South Atlantic* (eds. G. Fischer and G. Wefer), pp. 469–488. Springer-Verlag, Berlin, Germany.
- Badger M. R., Basset M., and Comins H. N. (1985) A model for HCO_3^- accumulation and photosynthesis in the cyanobacterium *Synechococcus* sp. *Plant Physiol.* **77**, 465–471.
- Bard E., Rostek F., and Sonzogni C. (1997) Interhemispheric synchrony of the last deglaciation inferred from alkenone paleothermometry. *Nature* **385**, 707–710.
- Bendle J. A. and Rosell-Melé A. (2001) *Appraisal of alkenone indices as temperature and salinity proxies in the Gin seas and Holocene millennial-scale sea surface variability on the Icelandic shelf*. Paper presented at the 7th International Conference on Paleoceanography, September 16–22, Sapporo, Japan.
- Bentaleb I., Fontugne M., Descolas-Gros C., Girardin C., Mariotti A., Pierre C., Brunet C., and Poisson A. (1996) Organic carbon isotopic composition of phytoplankton and sea-surface pCO_2 reconstructions in the Southern Indian Ocean during the last 50,000 yr. *Org. Geochem.* **24**, 399–410.
- Bidigare R. R., Fluegge A., Freeman K. H., Hanson K. L., Hayes J. M., Hollander D., Jasper J. P., King L. L., Laws E. A., Milder J., Millero F. J., Pancost R., Popp B. N., Steinberg P. A., and Wakeham S. G. (1997) Consistent fractionation of ^{13}C in nature and in the laboratory: Growth rate in some haptophyte algae. *Global Biogeochem. Cycles* **11**, 279–292.

- Brassell S. C., Eglinton G., Marlowe I. T., Pflaumann U., and Sarnthein M. (1986) Molecular stratigraphy: A new tool for climatic assessment. *Nature* **320**, 129–133.
- Conte M. H., Eglinton G., and Madureira L. A. S. (1992) Long-chain alkenones and alkyl alkenoates as paleotemperature indicators: Their production, flux and early sedimentary diagenesis in the eastern North Atlantic. *Org. Geochem.* **19**, 287–298.
- Conte M. H., Thompson A., and Eglinton G. (1994a) Primary production of lipid biomarker compounds by *Emiliania huxleyi*. Results from an experimental mesocosm study in fjords of southwestern Norway. *Sarsia* **79**, 319–331.
- Conte M. H., Volkman J. K., and Eglinton G. (1994b) Lipid biomarkers of the haptophyta. In *The Haptophyte Algae*, Systematics Association Special Volume No. 51 (eds. J. C. Green and B. S. C. Leadbeater), pp. 351–377, Clarendon Press, Oxford, UK.
- Conte M. H., Thompson A., Eglinton G., and Green J. C. (1995) Lipid biomarker diversity in the coccolithophorid *Emiliania huxleyi* (prymnesiophyceae) and the related species *Gephyrocapsa oceanica*. *J. Phycol.* **31**, 272–282.
- Conte M. H., Weber J. C., King L. L., and Wakeham S. G. (2001) The alkenone temperature signal in western North Atlantic surface waters. *Geochim. Cosmochim. Acta* **65**, 4275–4287.
- Craig H. (1970) Abyssal carbon 13 in the South Pacific. *J. Geophys. Res.* **75**, 691–695.
- Doose H., Prahl F. G., and Lyle M. W. (1997) Biomarker temperature estimates for modern and last glacial surface waters of the California Current system between 33° and 42°N. *Paleoceanography* **12**, 615–622.
- Edge J. K. and Heimdal B. R. (1994) Blooms of phytoplankton including *Emiliania huxleyi* (haptophyta). Effects of nutrient supply in different N:P ratios. *Sarsia* **79**, 333–348.
- Epstein B. L., D'Hondt S., Quinn J. G., Zhang J., and Hargraves P. E. (1998) An effect of dissolved nutrient concentrations on alkenone-based temperature estimates. *Paleoceanography* **13**, 122–126.
- Epstein B. L., D'Hondt S., and Hargraves P. E. (2001) The possible metabolic role of C₃₇ alkenones in *Emiliania huxleyi*. *Org. Geochem.* **32**, 867–875.
- François R., Altabet M. A., Goericke R., McCorkle D. C., Brunet C., and Poisson A. (1993) Changes in the δ¹³C of surface water particulate organic matter across the subtropical convergence in the SW Indian Ocean. *Global Biogeochem. Cycles* **7**, 627–644.
- Freeman K. H. and Wakeham S. G. (1992) Variations in the distributions and isotopic compositions of alkenones in Black Sea particles and sediments. *Org. Geochem.* **19**, 277–285.
- Gong C. and Hollander D. J. (1999) Evidence for differential degradation of alkenones under contrasting bottom water oxygen conditions: Implication for paleotemperature reconstruction. *Geochim. Cosmochim. Acta* **63**, 405–411.
- Goñi M. A., Hartz D. M., Thunell R. C., and Tappa E. (2001) Oceanographic considerations for the application of the alkenone-based paleotemperature U^K₃₇ index in the Gulf of California. *Geochim. Cosmochim. Acta* **65**, 545–557.
- Herbert T. D. (2001) Review of alkenone calibrations. (culture, water column, and sediments). *Geochem. Geophys. Geosyst.* **2**, paper #2000GC000055.
- Iida K. and Saito S. (2001) Study on temporal and lateral variation of the spring bloom in the Bering Sea by using multi-sensor remote sensing. In *The Spring Meeting of the Oceanographic Society of Japan*, p. 233 (in Japanese).
- Ishiwatari R., Houtatsu M., and Okada H. (2001) Alkenone-sea surface temperatures in the Japan Sea over the past 36 kyr: Warm temperatures at the last glacial maximum. *Org. Geochem.* **32**, 57–67.
- Jasper J. P. and Hayes J. M. (1990) A carbon isotope record of CO₂ levels during the late Quaternary. *Nature* **347**, 462–464.
- Jasper J. P., Hayes J. M., Mix A. C., and Prahl F. G. (1994) Photosynthetic fractionation of ¹³C and concentrations of dissolved CO₂ in the central equatorial Pacific during the last 255,000 years. *Paleoceanography* **9**, 781–798.
- Johnston A. M. (1996) The effect of environmental variables on ¹³C discrimination by two marine phytoplankton. *Mar. Ecol. Prog. Ser.* **132**, 257–263.
- Komai N. and Wataki K. (2000) Dissolved oxygen measurement. In *R/V Mirai MR00-K06 Cruise Report* (ed. T. Takizawa), pp. 138–146. Japan Marine Science and Technology Center, Yokosuka City, Japan.
- Li J., Philp R. P., Pu F., and Allen J. (1996) Long-chain alkenones in Qinghai Lake sediments. *Geochim. Cosmochim. Acta* **60**, 235–241.
- Marlowe I. T., Brassell S. C., Eglinton G., and Green J. C. (1984a) Long chain unsaturated ketones and esters in living algae and marine sediments. *Org. Geochem.* **6**, 135–141.
- Marlowe I. T., Green J. C., Neal A. C., Brassell S. C., Eglinton G., and Course P. A. (1984b) Long chain (n-C₃₇-C₃₉) alkenones in the prymnesiophyceae: Distribution of alkenones and other lipids and their taxonomic significance. *Br. Phycol. J.* **19**, 203–216.
- Mizobata K., Miyamura T., Shiga N., Imai K., Toraya M., Kajiwara Y., Sasaoka T., and Saito S. (2001) Cross-section observation of eddies in the shelf-edge area of the southeastern Bering Sea. In *The Spring Meeting of the Oceanographic Society of Japan*, p. 231 (in Japanese).
- Mook W. G., Bommerson J. C., and Staberman W. H. (1974) Carbon isotope fractionation between dissolved bicarbonate and gaseous carbon dioxide. *Earth Planet. Sci. Lett.* **22**, 169–176.
- Müller P. J., Kirst G., Rhuland G., von Storch I., and Rosell-Melé A. (1998) Calibration of the alkenone paleotemperature index U^K₃₇ based on core-tops from the eastern South Atlantic and the global ocean (60°N-60°S). *Geochim. Cosmochim. Acta* **62**, 1757–1772.
- Murata A. and Takizawa T. (2002) Impact of a coccolithophorid bloom on the CO₂ system in surface waters of the eastern Bering Sea shelf. *Geophys. Res. Lett.* **29**, 42–1–42–4.
- Nagata T., Fukuda R., Fukuda H., and Koike I. (2001) Basin-scale geographic patterns of bacterioplankton biomass and production in the subarctic Pacific, July–September 1997. *J. Oceanogr.* **57**, 301–313.
- Nanninga H. J. and Tyrrell T. (1996) The importance of light for the formation of algal blooms by *Emiliania huxleyi*. *Mar. Ecol. Prog. Ser.* **136**, 195–203.
- Napp J. M. and Hunt G. L. Jr. (2001) Anomalous conditions in the south-eastern Bering Sea 1997: Linkages among climate, weather, ocean, and biology. *Fish. Oceanogr.* **10**, 61–68.
- Odate T. and Saito S. (2001) Chlorophyll specific growth rate and grazing mortality rate of phytoplankton in the shelf water of the Bering Sea in summer. *Polar Biosci.* **14**, 122–128.
- Ohkouchi N., Kawamura K., Kawahata H., and Okada H. (1999) Depth ranges of alkenone production in the central Pacific Ocean. *Global Biogeochem. Cycles* **13**, 695–704.
- Ostermann D. (2001) Iceland sea carbonate flux increases dramatically. In *Woods Hole Oceanographic Institution Annual Report*, pp. 17–18. Woods Hole Oceanographic Institution Annual Report, Woods Hole, MA.
- Pagani M., Arthur M. A., and Freeman K. H. (1999) Miocene evolution of atmospheric carbon dioxide. *Paleoceanography* **14**, 273–292.
- Pelejero C. and Grimalt J. O. (1997) The correlation between the U^K₃₇ index and sea surface temperatures in the warm boundary: The South China Sea. *Geochim. Cosmochim. Acta* **61**, 4789–4797.
- Pelejero C. and Grimalt J. O. (1999) High-resolution U^K₃₇ temperature reconstructions in the South China Sea over the past 220 kyr. *Paleoceanography* **14**, 224–231.
- Popp B. N., Kenig F., Wakeham S. G., Laws E. A., and Bidigare R. R. (1998a) Does growth rate affect ketone unsaturation and intracellular carbon isotopic variability in *Emiliania huxleyi*? *Paleoceanography* **13**, 35–41.
- Popp B. N., Laws E. A., Bidigare R. R., Dore J. E., Hanson K. L., and Wakeham S. G. (1998b) Effect of phytoplankton cell geometry on carbon isotopic fractionation. *Geochim. Cosmochim. Acta* **62**, 69–77.
- Prahl F. G. and Wakeham S. G. (1987) Calibration of unsaturation patterns in long-chain ketone compositions for paleotemperature assessment. *Nature* **330**, 367–369.
- Prahl F. G., Muehlhausen L. A., and Zahnle D. L. (1988) Further evaluation of long-chain alkenones as indicators of paleoceanographic conditions. *Geochim. Cosmochim. Acta* **52**, 2303–2310.
- Rau G. H., Riebesell U., and Wolf-Gladrow D. (1997) CO₂aq-dependent photosynthetic ¹³C fractionation in the ocean: A model versus measurements. *Global Biogeochem. Cycles* **11**, 267–278.

- Riebesell U., Zondervan I., Rost B., Tortell P. D., Zeebe R. E., and Morel F. M. M. (2000a) Reduced calcification of marine plankton in response to increased atmospheric CO₂. *Nature* **407**, 364–367.
- Riebesell U., Revill A. T., Holdsworth D. G., and Volkman J. K. (2000b) The effects of varying CO₂ concentration on lipid composition and carbon isotope fractionation in *Emiliania huxleyi*. *Geochim. Cosmochim. Acta* **64**, 4179–4192.
- Riegman R., Noordeloos A. A. M., and Cadee G. C. (1992) Phaeocystis blooms and eutrophication of the continental coastal zones of the North Sea. *Mar. Biol.* **112**, 479–484.
- Rosell-Melé A. (1998) Interhemispheric appraisal of the value of alkenone indices as temperature and salinity proxies in high-latitude locations. *Paleoceanography* **13**, 694–703.
- Rosell-Melé A., Comes P., Müller P. J., and Ziveri P. (2000) Alkenone fluxes and anomalous U^K₃₇ values during 1989–1990 in the North-east Atlantic (48°N 21°W). *Mar. Chem.* **71**, 251–264.
- Sato K., Yokogawa S., Tanaka T., and Murata A. (2001) Nutrient measurements. In *R/V MIRAI MR00-K06 Cruise Report* (ed. T. Takizawa), pp. 147–165. Japan Marine Science and Technology Center, Yokosuka City, Japan.
- Shin K.-H., Tanaka N., Harada N., and Marty J.-C. (2002) Production and turnover rates of C₃₇ alkenones in the eastern Bering Sea: Implication for the mechanism of a long duration of *Emiliania huxleyi* bloom. *Prog. Oceanogr.* **55**, 113–129.
- Sicre M.-A., Ternois Y., Miquel J.-C., and Marty J.-C. (1999) Alkenones in the northwestern Mediterranean Sea: Interannual variability and vertical transfer. *Geophys. Res. Lett.* **26**, 1735–1738.
- Sicre M.-A., Bard E., Ezat U., and Rostek F. (2002) Alkenone distributions in the North Atlantic and Nordic sea surface waters. *Geochem. Geophys. Geosyst.* **3**:2, paper #2001GC000159.
- Sikes E. L. and Volkman J. K. (1993) Calibration of alkenone unsaturation ratios (U^K₃₇) for paleotemperature estimation in cold polar waters. *Geochim. Cosmochim. Acta* **57**, 1883–1889.
- Sikes E. L., Volkman J. K., Robertson L. G., and Pichon J.-J. (1997) Alkenones and alkenes in surface waters and sediments of the Southern Ocean: Implications for paleotemperature estimation in polar regions. *Geochim. Cosmochim. Acta* **61**, 1495–1505.
- Sonzogni C., Bard E., Rostek F., Dollfus D., Rosell-Melé A., and Eglinton G. (1997) Temperature and salinity effects on alkenones ratios measured in sediments from the Indian Ocean. *Quat. Res.* **47**, 344–355.
- Springer A. M., McRoy C. P., and Flint M. Y. (1996) The Bering Sea green belt: Shelf-edge processes and ecosystem production. *Fish Oceanogr.* **5**, 205–223.
- Stabeno P. J. and Van Meurs P. (1999) Evidence of episodic on-shelf flow in the southeastern Bering Sea. *J. Geophys. Res.* **104**, (C12), 29715–29720.
- Stabeno P. J., Bond N. A., Kachel N. B., Salo S. A., and Schumacher J. D. (2001) On the temporal variability of the physical environment over the south-eastern Bering Sea. *Fish Oceanogr.* **10**, 81–98.
- Stockwell D. A., Whilkedge T. E., Zeeman S. I., Coyle K. O., Napp J. M., Brodeur R. D., Pinchuk A. I., and Hunt G. L. Jr. (2001) Anomalous conditions in the south-eastern Bering Sea, 1997: Nutrients, phytoplankton and zooplankton. *Fish Oceanogr.* **10**, 99–116.
- Tanaka N., Shin K. H., Tanaka T., and Narita H. (2001) Observation of a coccolithophorid bloom on the continental shelf of the Bering Sea in 2000. In *The Spring Meeting of the Oceanographic Society of Japan*, p. 234 (in Japanese).
- Teece M. A., Getlife J. M., Leftley J. W., Parkes R. J., and Maxwell J. R. (1998) Microbial degradation of the marine prymnesiophyte *Emiliania huxleyi* under oxic and anoxic conditions as a model for early diagenesis: Long chain alkadienes, alkenones and alkyl alkenoates. *Org. Geochem.* **29**, 863–880.
- Ternois Y., Sicre M.-A., Boireau A., Conte M. H., and Eglinton G. (1997) Evaluation of long-chain alkenones as paleo-temperature indicators in the Mediterranean Sea. *Deep-Sea Res.* **44**, 271–286.
- Ternois Y., Kawamura K., Keigwin L., Ohkouchi N., and Nakatsuka T. (2001) A biomarker approach for assessing marine and terrigenous inputs to the sediments of Sea of Okhotsk for the last 27,000 years. *Geochim. Cosmochim. Acta* **65**, 791–802.
- Townsend D. W., Leller M. D., Holligan P. M., Ackleson S. G., and Balch W. M. (1994) Blooms of the coccolithophore *Emiliania huxleyi* with respect to hydrography in the Gulf of Maine. *Continental Shelf Res.* **14**, 979–1000.
- Tyrell T. and Taylor A. H. (1996) A modeling study of *Emiliania huxleyi* in the NE Atlantic. *J. Mar. Syst.* **9**(1/2), 83–112.
- US National Oceanographic Data Center. (1998) *World Ocean Atlas 1998*. Available: http://www.nodc.noaa.gov/OC5/WOA98F/woaf_cd/search.html
- Versteegh G. J. M., Riegman R., de Leeuw J. W., and Jansen J. H. F. (2001) U^K₃₇ values for *Isochrysis galbana* as a function of culture temperature, light intensity and nutrient concentrations. *Org. Geochem.* **32**, 785–794.
- Volkman J. K. (2000) Ecological and environmental factors affecting alkenone distributions in seawater and sediments. *Geochem. Geophys. Geosyst.* **1**, paper #2000GC000061.
- Volkman J. K., Eglinton G., Corner E. D. S., and Sargent J. R. (1980) Novel unsaturated straight-chain C37-C39 methyl and ethyl ketones in marine sediments and a coccolithophorid *Emiliania huxleyi*. In *Advances in Organic Geochemistry* (eds. A. G. Doullas and J. R. Maxwell), pp. 219–227. Pergamon, New York.
- Weaver P. P. E., Chapman M. R., Eglinton G., Zhao M., Rutledge D., and Read G. (1999) Combined coccolith, foraminiferal, and biomarker reconstruction of paleoceanographic conditions over the past 120 kyr in the northern North Atlantic (59°N, 23°W). *Paleoceanography* **14**, 336–349.
- Younker M. B., MacDonald R. W., Veltkamp D. J., and Cretney W. J. (1995) Terrestrial and marine biomarkers in a seasonally ice-covered Arctic estuary: Integration of multivariate and biomarker approaches. *Mar. Chem.* **49**, 1–50.